Journal of Photonics for Energy

SPIEDigitalLibrary.org/jpe

Micro-optical design of photochemical upconverters for thin-film solar cells

Tim F. Schulze
Yuen Yap Cheng
Tony Khoury
Maxwell J. Crossley
Bernd Stannowski
Klaus Lips
Timothy W. Schmidt

SPIE

Micro-optical design of photochemical upconverters for thin-film solar cells

Tim F. Schulze,[a] Yuen Yap Cheng,[a] Tony Khoury,[a] Maxwell J. Crossley,[a] Bernd Stannowski,[b] Klaus Lips,[c] and Timothy W. Schmidt[a]

[a]The University of Sydney, School of Chemistry, NSW 2006, Australia
timothy.schmidt@sydney.edu.au
[b]Competence Centre Thin Film and Nanotechnology for Photovoltaics Berlin (PVcomB), Helmholtz-Zentrum Berlin für Materialien und Energie, 12489 Berlin, Germany
[c]Institute for Silicon Photovoltaics, Helmholtz-Zentrum Berlin für Materialien und Energie, 12489 Berlin, Germany

Abstract. All presently available types of solar cells transmit light with energies below their band gaps, foregoing energy. An elegant way toward overcoming these subbandgap losses and using a larger fraction of the incident light is the re-shaping of the solar spectrum by upconversion (UC) of photons. Recently, first results on solar cells augmented by either lanthanide-based UC or triplet-triplet-annihilation UC in organic chromophores were presented. Both of these UC strategies are characterized by a nonlinear response on the illumination density under conditions relevant to solar energy conversion, opening a route for increasing the UC yield by concentrating the light. While operation of the whole cell under concentrated sunlight is in most cases undesirable, application of micro-optical focusing of the transmitted light in the upconverting layer is a promising strategy. In the present work, a more than two-fold enhancement of the current gain by UC behind an amorphous silicon solar cell through optimization of the upconverter optical design is demonstrated, including employing a focusing microstructured back reflector. The experimental data is rationalized using a simple ray tracing modeling approach, highlighting a further enhancement potential of a microstructured UC unit. © *2013 Society of Photo-Optical Instrumentation Engineers (SPIE)* [DOI: 10.1117/1.JPE.3.034598]

Keywords: third-generation photovoltaics; thin film solar cells; upconversion.

Paper 12062 received Oct. 22, 2012; revised manuscript received Jan. 16, 2013; accepted for publication Jan. 16, 2013; published online Feb. 6, 2013; corrected Feb. 8, 2013.

1 Introduction

Single threshold solar cells are limited to an energy conversion efficiency of about 33% under one sun, the well-known Shockley-Queisser limit.[1,2] For cells with higher band gaps, such as thin film silicon and organic photovoltaics, the limit is even lower, with significant fractions of the solar spectrum being transmitted unused. Indeed, these "subbandgap losses" represent the most severe loss mechanism for those thin-film cells.[3] But even solar cells made from crystalline silicon sacrifice a considerable part of the solar spectrum. The subbandgap losses can be remedied by the application of upconversion (UC), whereby transmitted (infra)red light is converted to light of higher energy, which can then be harvested by the cell and contribute to current generation. Based on detailed balance considerations it was shown that UC could boost the maximum energy conversion efficiency to about 44% for a solar cell with a bandgap of 1.6 eV.[4] Crystalline silicon cells could still reach about 38%, although the potential gain is smaller than for the high-bandgap devices.

In recent years, UC has been an active area in the field of "third-generation photovoltaics" which comprises all device concepts that are, in principle, capable of circumventing the Shockley-Queisser limit.[5,6] Research has focused mainly on two different and mainly complementary approaches.[7] First, the application of lanthanide cations (mostly erbium and ytterbium)

0091-3286/2013/$25.00 © 2013 SPIE

in a solid-state matrix, making use of their discrete and long-lived atomic states that can facilitate multiphoton absorption, followed by upconverted phosphorescence. The rare-earth materials absorb in the infrared region of the solar spectrum as far down as 1500 nm and lanthanide UC (L-UC) is thus interesting for application to c-Si solar cells.[8,9]

The second active field of research is the application of organic chromophores in solution, undergoing triplet-triplet-annihilation UC (TTA-UC).[10] Here, one class of molecules (sensitizers) stores the energy obtained by absorption of a low-energy photon in a long-lived triplet state. Triplet electronic energy transfer to a second molecule (emitter), present in excess, occurs by bimolecular collisions. Then, upon collision of two thus excited emitters, TTA occurs which produces fluorescence from one emitter molecule at higher photon energy then initially absorbed while the other collapses to its ground state in the TTA event. These materials work efficiently in the red and near infrared part of the spectrum and are thus interesting for high-bandgap thin-film solar cells.

Recently, significant progress was demonstrated in the application of both concepts to actual solar cells in their respective domains:L-UC was applied to c-Si[9,11] and a-Si:H[12] solar cells, while TTA-UC was employed in a-Si:H[13,14] and organic bulk heterojunction solar cells.[15] TTA-UC seems to have generic advantages over L-UC, mainly due to the much higher absorption strength of the organic chromophores, and peak quantum yields of the UC process of 30% (with 50% being the maximum).[16] Current enhancements of up to 7×10^{-4} mA/cm^2 were measured in a-Si:H cells with TTA-UC,[15] while L-UC is still limited to about 7×10^{-7} mA/cm^2 for this type of cell. Nonetheless, the two approaches can be seen as being complimentary for their operating in different spectral regions, and the recently presented approach of dye-sensitized lanthanide UC may increase the UC yield in the lanthanide systems. [17]

Both aforementioned mechanisms are characterized by a quadratic dependence of the UC yield on the illumination density under the low-light conditions relevant to solar energy conversion, which results from the necessity of two excited states coinciding in space and time, for UC to happen.[18–20] This in principle opens an interesting field for optical design of solar cell/upconverter assemblies, as any concentration of light potentially increases the UC yield. Plasmonics have been investigated to this end due to the intense local electric field associated with a plasmon resonance, which however is confined to the immediate vicinity of metal nanostructures.[21] Thus, plasmonics can only effectively augment UC processes if the absorption strength of the upconverting medium is high enough, i.e., the concentration of upconverting molecules/lanthanide ions, so as to make use of high E field strength in regions of only some tens of nanometers extent. So far, however, for both TTA-UC and L-UC, the absorption is weaker by orders of magnitude, and in consequence, plasmonically enhanced UC has only been studied on model systems not applicable to devices (e.g., in reflection[21]). Indeed, in the currently predominant regime of characteristic absorption lengths well above the wavelength in the upconverting materials, far-field optical means for concentration are a much more promising approach.

In this report, we demonstrate how the choice of an appropriate thickness of upconverting medium in combination with a suitable back-reflector leads to a doubling of the UC contribution to the current output of an amorphous silicon thin-film solar cell. We further introduce a focusing back-reflector as obtained by an array of spherical imprints in a metal coated polytetrafluoroethylene (PTFE) film, which leads to an additional increase of the photocurrent. Using a simple ray tracing modeling approach, we demonstrate that the potential of such microstructured back-reflector is a total nine-fold enhancement of the UC yield, while at the same time improving the overall external quantum efficiency (EQE) of the solar cell. Such microstructured design is thus highlighted to be promising for solar cell implementation of upconverting materials with characteristic absorption lengths above the μm range.

2 Experimental Details

The study was conducted with an *in situ* approach, measuring the EQE of an amorphous silicon *p-i-n* solar cell with an upconverting layer of variable thickness sandwiched between the glass substrate of the solar cell and an exchangeable back reflector. This configuration was realized in

a variable "half cuvette", where the solar cell glass substrate forms one side of a variable cavity inside a vacuum-tight container that is directly attached to the solar cell while an O-ring provides sealing (Fig. 1, schematic on the left, picture on the right). Micrometer screws allowed variation of the thickness of the upconverting layer with a precision better than ± 10 μm, by closing the gap between the back reflector and the glass substrate. By measuring the impact of the upconverter optical configuration (thickness, nature of back-reflector) on the solar cell spectral response, we can use the photocurrent as an unequivocal measure of the optical performance of the upconverting solar cell backside.

The upconverting layer consists of a well-characterized combination of organic chromophores undergoing TTA-UC. We employed {5,10,15,20-tetrakis(3,5-di-*tert*-butylphenyl)tetrakisquinoxalino[2,3-b′:7,8-b″,12,13-b‴:17,18-b⁗]porphyrinato}palladium(II), abbreviated as PQ_4Pd, as sensitizer molecule at a concentration of 7 to 9×10^{-4} M, and rubrene as emitter at 5×10^{-3} M, dissolved in toluene.[13,22] The molecular structures of these compounds are depicted in Fig. 2(a). The UC principle, as described in detail elsewhere,[4,10] is depicted in Fig. 2(b) and can be summarized as follows: after absorption of a low energy photon with energy $h\nu_1$, the sensitizer molecule undergoes immediate intersystem crossing (ISC) to its first excited triplet state T_1. Ensuring fast triplet electronic energy transfer (TET) stores this energy in the first triplet state of the emitter molecule, sacrificing a small amount of energy to drive the transfer process. Two colliding emitters then facilitate triplet-triplet annihilation (TTA), bringing about one emitter molecule in its first excited singlet state, S_1, which leads to fluorescence at energy, $h\nu_2$. For this process to proceed with the highest efficiency, oxygen has to be excluded as its singlet state is easily accessed from the sensitizer triplet, T_1, leading to loss of excitons and the formation of highly corrosive singlet oxygen. This was done by three freeze-pump-thaw cycles employing liquid nitrogen cooling and a diffusion pump stage with a base pressure of $<5 \times 10^{-7}$ mbar.

The solar cell was a state-of-the-art a-Si:H *p-i-n* cell on a glass substrate with transparent contacts made of Al-doped ZnO, having a maximum conversion efficiency of 7.5% (initial) when illuminated through the glass substrate under presence of a simple Lambertian back-reflector (white paint). With illumination through the ZnO/(n)a-Si:H back contact as used for the UC measurements, 3.9% was measured. Details on the solar cell processing can be found elsewhere.[15]

Due to the mentioned quadratic dependence of the UC yield on the illumination density, the UC signal at the low illumination levels employed in usual solar cell EQE setups is negligible.

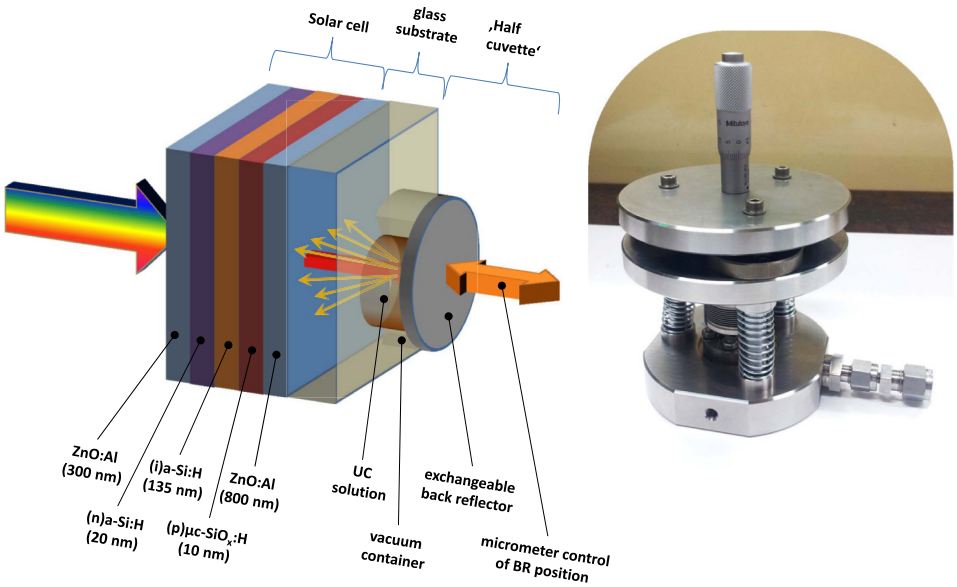

Fig. 1 Schematic of the experimental setup. Right side: picture of the half cuvette that allows precise control of the layer thickness of the upconverting medium, while it is in direct contact with the solar cell glass substrate.

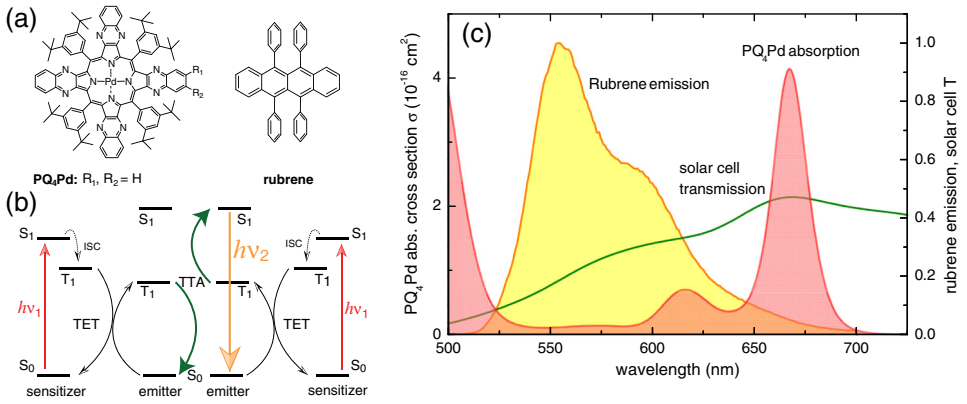

Fig. 2 (a) Molecular structures of sensitizer (PQ_4Pd) and emitter (rubrene species). (b) Schematic of the energy levels and processes involved in triplet-triplet annihilation upconversion. (c) Spectral alignment of PQ_4Pd absorption (red) and rubrene emission characteristics (yellow), as well as the a-Si:H solar cell transmission curve (green).

To be able to observe a clear signal from UC in the solar cell EQE, we therefore illuminate the upconverter by a continuous laser beam at the peak absorption wavelength of the sensitizer (670 nm) incident on the solar cell during the EQE measurement, in order to create a background triplet concentration and thus increase the yield of upconverted photons. Note that due to the lock-in detection method of the EQE measurement employing a chopped probe beam, the continuous 670 nm pump does not affect the EQE measurement. As the absorption of the solar cells in this spectral range is weak, the photocurrent itself is also not significantly biased by the red laser. However, to eliminate any possible effect of the 670 nm bias on the solar cell response, we did not switch off the laser to measure the EQE without UC contribution, but laterally displaced the 670 nm pump beam on the active area, thus misaligning it with the EQE probe beam. Thereby, the solar cell still sees the same illumination conditions, but within the area probed by the EQE measurement the contribution of UC to the linear response is negligible. A sketch of the EQE setup is depicted in Fig. 3, showing the aligned laser and probe beam.

To calculate the effective number of suns imposed by this light bias we matched the sensitizer excitation rate by the 670 nm laser to that which would be present under a certain concentration of the AM1.5G spectrum, as filtered by the solar cell. The rate of excitation of the sensitizer molecules, k_Φ, by one sun is calculated by multiplication of the AM1.5G solar spectrum, $\Phi_{AM1.5G}$ in photons $cm^{-2}\ s^{-1}\ nm^{-1}$ by the transmission of the solar cell, T_{SC}, and integrating the product of this with the sensitizer absorption cross section, σ, in cm^2,

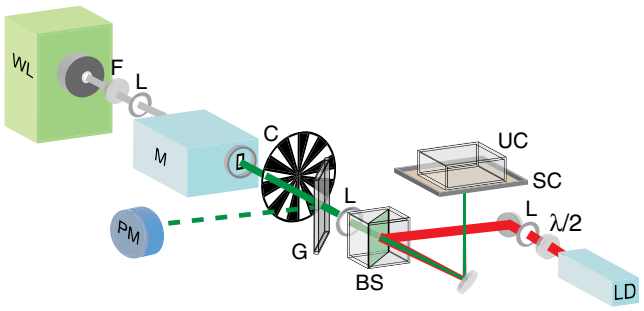

Fig. 3 EQE setup as used to measure the upconversion-augmented solar cells. Light from a white-light source (WL) is long-pass filtered (F), monochromated (M), chopped at 118 Hz (C) and focused by lenses (L) onto the solar cell/upconverter unit. A glass slide (G) is used to couple part of the light onto a photodiode power meter (PM) to monitor its intensity. 670 nm light from a laser diode (LD) is focused onto the same spot on the solar cell by means of lenses (L) and a beam splitter (BS). A $\lambda/2$ plate is used to control the polarization and thus the reflectance of the BS. The contribution of the 670 nm light bias and chopped EQE probe beam to the solar cell current signal are deconvoluted by means of lock-in detection.

$$k_\Phi = \int \Phi_{\mathrm{AM1.5G}}(\lambda) T_{\mathrm{SC}}(\lambda) \sigma(\lambda) \mathrm{d}\lambda. \tag{1}$$

We calculated $k_\Phi = 2.4\ \mathrm{s}^{-1}$ for the present a-Si:H solar cells. The irradiation density I_b of the bias laser in photons $\mathrm{cm}^{-2}\ \mathrm{s}^{-1}$ is used to calculate the experimental pump rate, i.e., $k_b = \sigma(670\ \mathrm{nm})\ T_{\mathrm{SC}}(670\ \mathrm{nm})\ I_b$. The ratio $C = k_\Phi / k_b$ then gives the effective solar concentration C, which was about 47 to 55 suns in the present case.

We compare the solar cell performance with and without upconverter by taking the ratio between the EQE taken with the 670 nm beam aligned with the EQE probe beam ($\mathrm{EQE_{UC}}$) and the EQE with misaligned UC pump beam ($\mathrm{EQE_0}$).

3 Results and Discussion

3.1 *Specular Mirror as Back-Reflector*

In a first step, we employed a planar mirror (polished glass slide coated with silver) as a back-reflector behind the upconverting solution. We varied the thickness of the upconverting layer between 4.5 mm, which was the maximum retracted position of the piston holding the mirror, and nominally zero as defined by the relative positioning of the back-reflector surface with respect to the sealing surface of the half cuvette as measured with a micrometer depth gauge prior to installation of the half cuvette on the solar cell. We started with the back-reflector positioned at 4.5 mm, measuring the solar cell EQE with aligned probe and pump beams (contribution by UC), and misaligned pump beam (no contribution by UC). Then, we decreased the thickness of the upconverter and repeated the sequence. After having reached nominally zero distance, we retracted the piston and re-measured the 4.5 mm position to verify that no baseline shift was present. Two spectra were taken with aligned and misaligned beams for each position of the back-reflector, and the average spectra for aligned beams ($\mathrm{EQE_{UC}}$) and misaligned beams ($\mathrm{EQE_0}$) were then analyzed further. Details on the measurement scheme can be found elsewhere.[13,14]

The analysis of EQE data consisted of fitting the ratio $\mathrm{EQE_{UC}}/\mathrm{EQE_0}$ with an equation describing the expected UC signal in the EQE,[14] which reads

$$\frac{\mathrm{EQE_{UC}}(\lambda)}{\mathrm{EQE_0}(\lambda)} = 1 + \chi \frac{T_{\mathrm{SC}}(\lambda)}{\mathrm{EQE_0}} \frac{\sigma(\lambda)\sigma_b}{\sigma(\lambda) + \sigma_b}, \tag{2}$$

with σ_b being the porphyrin absorption cross section at the bias laser wavelength (670 nm), and the free parameter χ accounting for the efficiency of the upconverter and its optical coupling to the solar cell. Fitting this function to the EQE ratio yields excellent fits, as can be observed in Fig. 4(a).

Plotting the values for χ, normalized to the value at 4.5 mm approximating the limit of "infinite thickness," against the thickness of the upconverting layer in Fig. 4(b), we observe a pronounced peak at around 60 μm thickness of the upconverter, where an enhancement factor of about 1.8 times is reached. For thicknesses smaller than these 60 μm, the signal is dropping steeply, while a slow decrease is observed for larger thicknesses [note the logarithmic abscissa in Fig. 4(b)].

3.2 *Ray Tracing Simulations*

To comprehend the trend of Fig. 4(b), we performed optical simulations of the upconverter behind the a-Si:H solar cell, in the presence of a specular back-reflector. We set up a three-dimensional (3-D) ray-tracing simulation coupled to the rate equations describing the UC process. Although a 3-D approach is not necessary to model the behavior of the upconverter in the presence of a flat back-reflector, we take that approach here to be able to generalize to structured back-reflectors, to be discussed in the next section.

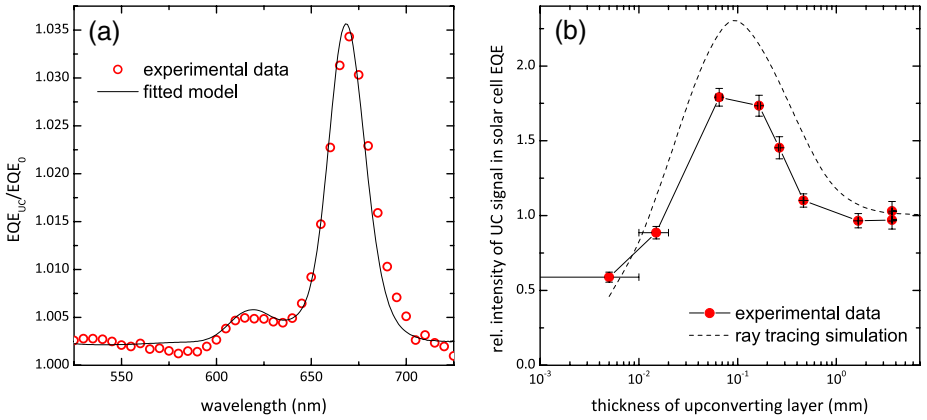

Fig. 4 (a) Example of the upconversion signature in the EQE ratio EQE_{UC}/EQE_0, and the respective single-parameter fit of a model describing the expected signal in EQE_{UC}/EQE_0. (b) Relative intensity of UC signal in solar cell EQE as a function of the upconverting layer.

3.2.1 *Incoming rays*

We start with the photon flux of the AM1.5G solar spectrum, $\Phi_{AM1.5G}$, which we multiply by the measured transmission of the solar cell, T_{SC}. This gives the spectral photon flux in $cm^{-2}\ nm^{-1}\ s^{-1}$ incident on the upconverter unit. We restrain the spectrum to the sensitizer absorption range (550 to 750 nm), and scale it by a suited number while rounding the photon numbers in each 1 nm bin to an integer, as to have a defined number of total photons in the spectral region of interest. Usual total numbers within 550 to 750 nm were in the 100,000 range, leading to several hundred photons for each nm, so that the rounding does not impact the general form of the spectrum.

The photons from each 1-nm bin of the incident spectrum must have a distinct distribution of penetration depths into the upconverting solution, which depends on the concentration of sensitizer molecules and their absorption coefficient at the respective wavelength. Here, we employed PQ_4Pd, whose absorption spectrum is depicted in Fig. 2(c). For the simulation we want to be able to map a random integer between 0 and 1 onto a ray length in such way that any random sample of rays approximates the correct distribution of ray lengths for the given wavelength. The fraction of rays absorbed within a length l at wavelength λ and for sensitizer concentration c_S is given by

$$p(l,\lambda,c_S) = \int_{x=0}^{l} c_S\sigma(\lambda)\exp[-c_S\sigma(\lambda)x], \tag{3}$$

with σ being the sensitizer absorption cross-section. The inverse function of this quantity gives us the length of a ray for a given "position" within the distribution of ray length, as is practically defined by a random number p between 0 and 1:

$$l(p,\lambda,c_S) = [p]^{-1} = \frac{\log(1-p)}{c_S\sigma(\lambda)}. \tag{4}$$

This equation yields the correct distribution of ray lengths for every wavelength within the spectrum of interest, for any random sample of numbers p. In the model, each ray also gets assigned a random position within the two-dimensional (2-D) plane defining the simulation area, defined by two additional random numbers, x and y. The algorithm now proceeds through the 1-nm bins of the incident spectrum, producing the correct number of rays for each bin, while assigning random positions and a length according to Eq. (4) to each ray.

Each simulation run is performed with a certain thickness a of the upconverting layer. Rays hitting the backside of the simulation volume are reflected with a probability which equals the assumed reflectivity of the backside, R_{BS}. Rays absorbed at the backside or exiting the simulation volume are not registered, while for all other rays the position of absorption is recorded in an array.

After all rays have been processed, bin counting is performed on the resulting array of positions, using a fixed bin size. Usually, $5 \times 5 \times 5\ \mu m^3$ bins were chosen, which was found to be a reasonable compromise between the coarseness of discretization of the simulation volume and small numbers of absorbed rays per bin, which would introduce scatter in the output data due to the nonlinear local response of the UC on the number of absorbed photons. We verified that the simulation results did not depend markedly on the choice of bin size.

3.2.2 *Local upconversion response*

Knowing the local rate of photon absorption allows calculating the excitation rate k_Φ of the sensitizer molecules, by dividing the number of photons absorbed in the respective bin in every second by the number of sensitizer molecules in the bin, taking into account the sensitizer concentration c_S. Then, the local UC efficiency can be calculated from the rate equations describing the triplet-triplet-annihilation process. For the description of TTA-UC it is usually assumed that the transfer of the triplet energy from the excited sensitizer to the emitter species, being present in the solution in excess, is immediate and not limiting the process. This assumption is backed by experimental evidence.[16,20,23] Then, the steady-state concentration of emitter molecules in their first excited triplet state, $[T]$, is given by

$$\frac{d[T]}{dt} = 0 = k_\Phi[S] - k_1[T] - k_{TTA}[T]^2, \tag{5}$$

with k_1 being the first-order decay constant of triplets (leading to loss of the energy stored in the triplet state), k_{TTA} being the (second-order) rate constant for triplet-triplet annihilation leading to upconverted fluorescence, and $[S]$ is the concentration sensitizer molecules. The steady-state solution of Eq. (5) is

$$[T] = \frac{-k_1 \pm \sqrt{k_1^2 + 4k_\Phi k_{\mathrm{TTA}}[S]}}{2k_{\mathrm{TTA}}}, \tag{6}$$

which allows us to calculate the fraction of excited emitter molecules decaying via TTA, given by

$$f_{\mathrm{TTA}} = \frac{k_{\mathrm{TTA}}[T]}{k_1 + k_{\mathrm{TTA}}[T]}. \tag{7}$$

It was found experimentally that the TTA quantum yield in the present system saturates at about 30% for high excitation fluence.[19] Note that the theoretical maximum is 50% due to the merging of two photons in the process of UC. For the simulation, we assumed the practical maximum quantum yield to be the experimentally found 30%, thus the UC quantum yield in dependence on the sensitizer excitation rate k_Φ is given by

$$Y_{\mathrm{TTA}}(k_\Phi) = 0.3 f_{\mathrm{TTA}} = 0.3 \frac{-k_1 + \sqrt{k_1^2 + 4k_\Phi k_{\mathrm{TTA}}[S]}}{k_1 + \sqrt{k_1^2 + 4k_\Phi k_{\mathrm{TTA}}[S]}}. \tag{8}$$

3.2.3 *Out-coupling of upconverted light*

The number of absorbed photons in every bin was converted to a number of emitted upconverted photons by multiplication with the local Y_{TTA} as obtained from the rate equations and taking measured values for k_1 and k_{TTA} ($k_1 = 10^{-4}\ s^{-1}$, $k_{\mathrm{TTA}} = 1.7 \times 10^{-13}\ cm^3\ s^{-1}$).[16,19] It has then to be taken into account that emission occurs isotropically, and that the photons can get reabsorbed on their way towards the solar cell by both the sensitizer and the emitter molecules. The reabsorption by the sensitizer molecules is more severe, as their absorption cross section is higher and the rubrene emitter fluorescence yield is close to unity, so photons reabsorbed by the emitter are most likely reemitted. Therefore, only the reabsorption by the sensitizer molecules was taken into account.

For each bin, the out-coupling efficiency was calculated for the geometrical conditions of the center of the bin. The calculation consisted in integrating the attenuation of the emitted fluence resulting from angle-dependent effective path lengths towards the solar cell over the entire emission sphere. For the hemisphere facing away from the solar cell, the rays were again assumed to be reflected at the back reflector with reflectivity R_{BS}. For the calculation of the attenuation, an average sensitizer absorption coefficient for the emission wavelength range was calculated, weighted with the normalized rubrene emission spectrum.

We assumed no reflection to occur at the interface between upconverter and the solar cell. The refractive index contrast between the solvent (toluene) and the solar cell's glass substrate is negligible, so reflection losses at this interface will be minimal. However, such losses could occur in the solar cell at the glass/ZnO and ZnO/a-Si:H interfaces. Yet it is difficult to quantify these losses as thin-film interference effects dominate the angle-dependent reflection properties of the solar cell: We performed calculations with a one-dimensional (1-D) transfer matrix formalism, but found the resulting reflection characteristics to be very sensitive to the assumed material properties of the ZnO and a-Si:H layers. Incorporating these simulated characteristics would thus have introduced some arbitrariness in the optical treatment concerning the choice of material parameters, while still missing some aspects such as roughness of the ZnO. For these reasons, we decided not to include reflectance at the solar cell internal surfaces. The photon output from the ray tracing calculations thus has to be seen as the limiting case for optimum coupling between solar cell and UC unit.

3.2.4 *Comparison to measurement*

In Fig. 4(b), the output of the ray tracing simulation is plotted along the experimental data. The parameters of the simulation were chosen to match the experimental conditions, and are listed in Table 1 (simulation run A). Observing Fig. 4(b), it is clear that the simulation captures the general trends of the photocurrent enhancement by UC upon variation of upconverter thickness quite well: For thicknesses much larger than the effective penetration depth $1\alpha = 1/(c_S\sigma)$), being about 60 μm for the sensitizer absorption peak in the present case, the incident rays are absorbed on a single pass. Further, the upconverted light is not efficiently coupled back into the solar cell as the part emitted towards the back-facing hemisphere is essentially lost. Closing the gap, some incident light hits the back reflector and contributes to effectively increasing the sensitizer excitation rate in the smaller volume. Although the overall volume participating in UC is decreased by closing the gap, the nonlinearity of the process leads to an overall gain of UC yield. Further, the emitted light is coupled back into the solar cell more efficiently when the path lengths of rays hitting the back reflector are getting smaller. The optimum is reached at about $d = 1/\alpha = 1/(c_S\sigma)$, when only 1/e of the incident light is absorbed upon the first pass. For even smaller distances, an increasing fraction of the light cannot be absorbed at all, which decreases the UC yield again.

The form of the enhancement curve and the peak position are captured well by the simulation, while the absolute amplitude of the enhancement as compared to the infinite limit is overestimated. This is most likely due to the missing treatment of reabsorption by the emitter species, in combination with an imperfect back reflector. In additional to potential losses by

Table 1 Simulation parameters of the ray tracing modeling.

Simulation run	Sphere diam. (μm)	iNdent. depth (μm)	C_{PQ_4Pd} (mmole)	R_{BS}	# suns	Bin size (μm)	# Rays	Embossed fraction f
A	50	20	0.66	0.96	55	5	100.000	0
B	50	20	0.9	0.88	47	5	100.000	0.33/0
C_1	50	20	0.9	0.88	1	5	100.000	0.33
C_2	50	20	0.9	0.96	1	5	100.000	0.33
C_3	50	20	0.9	0.96	1	5	100.000	0.77

nonradiative decay of thus excited rubrene (although as mentioned above, the rubrene fluorescence yield is high), reabsorption of upconverted light by the emitter will also increase the number of interactions between photons and the back reflector. This is because absorption and re-emission by the rubrene will more strongly affect the photons that have to travel longer distances in the upconverter, i.e., the ones emitted towards the back that potentially have already been reflected once. So this effect partly alleviates the beneficial effect of a back reflector and diminishes the amplitude of the enhancement peak.

As treating this effect explicitly would have complicated the ray tracing procedure considerably, we accept this shortcoming and bear in mind for the coming discussion that the simulation overestimates the enhancement by about 20%.

3.3 *Micro-Focusing by Embossed Metal-Coated PTFE*

The experimental evidence obtained with the planar silver mirror underlines the fact that any concentration of light leads to an increase of UC yield due to the nonlinearity of the UC response on illumination density. In the case presented above, a very moderate concentration was achieved only by multipassing the incoming light. It is thus suggested that much higher enhancements should be possible with a true optical focusing of the light.

To explore this idea in a simple proof-of-concept experiment, we have designed a structured back reflector featuring spherical indentations. Although a spherical dish provides a much less perfect focus than a parabolic mirror, an enhancement effect is to be expected, particularly for small indentation depths where the deviation from the parabolic form is not significant. The microstructure was achieved by hot-embossing of silica spheres into a 200-μm thick PTFE film according to a recipe.[24] To this end, a densely packed monolayer of 100 μm -diameter silica spheres was deposited on the sticky side of Kapton tape, which was then applied onto the PTFE film. The created sample was then heated to 170°C on a hotplate between two stainless steel disks lapped to a surface finish of <1 μm. After temperature equilibration of this stack, a pressure of 10 $\mathrm{kg/cm^2}$ was applied for 2 min for embossing. The resulting microstructure consisted of an array of spherical imprints of about 15 to 20 μm depth (70 to 80 μm diameter). The quality of the embossing result was verified with SEM images Fig. 3(a), while a focused-ion-beam cut through the center of one of the dimples verified their spherical shape and depth, and the diameter [Fig. 3(b)]. Finally, aluminum was evaporated onto the embossed PTFE film in a thermal evaporation apparatus (base pressure $<10^{-6}$ mbar). We chose a piece of the PTFE film that comprised both embossed and flat regions as back reflector for the next experiment and glued it onto a neodymium rare-earth magnet serving as the sample holder using instant adhesive.

The experiment again consisted of measuring the spectral response of an a-Si:H *p-i-n* solar cell with the half cuvette attached to the solar cell glass substrate, varying the distance of the back reflector and thus the thickness of the upconverting layer. We adjusted the lateral position of the EQE measurement such that in a first run, the embossed part of the back reflector was illuminated, while in a second run the flat region was probed. The amplitude of the UC signal in the solar cell EQE is plotted in Fig. 5(a) for both the embossed and flat back reflector. Both curves show a similar trend as found for the flat Ag reflector [Fig. 4(b)], i.e., for decreasing thickness of the UC layer, an increased UC signal is found and a successive decrease for very small distances. Interestingly, the UC signal taken with the embossed reflector peaks at smaller thickness and at reaches a higher peak value. Thus it is indeed found that the embossed reflector is superior to a flat reflector. For the EQE curves showing the largest UC contribution (embossed back reflector, 12 μm nominal thickness of UC unit), we calculated the photocurrent enhancement that would be brought about at 1 sun illumination by a procedure described elsewhere.[13,14] We obtained a value of about 5×10^{-4} $\mathrm{mA/cm^2}$, which is about 18 times higher than our previous result using the same sensitizer material,[13] and close to the highest current increase reported so far for a-Si:H solar cells which was obtained with a more broadly absorbing sensitizer.[15] This large improvement is partly due to a higher sensitizer concentration used in the present experiments (9×10^{-4} M as compared to 3.3×10^{-4} M) and better solar cells,[15] but a large part of the increase stems from the optimized optics.

Although the enhancement obtained by employing the embossed back reflector is moderate, higher improvements are to be expected with an optimized back reflector. To explore these

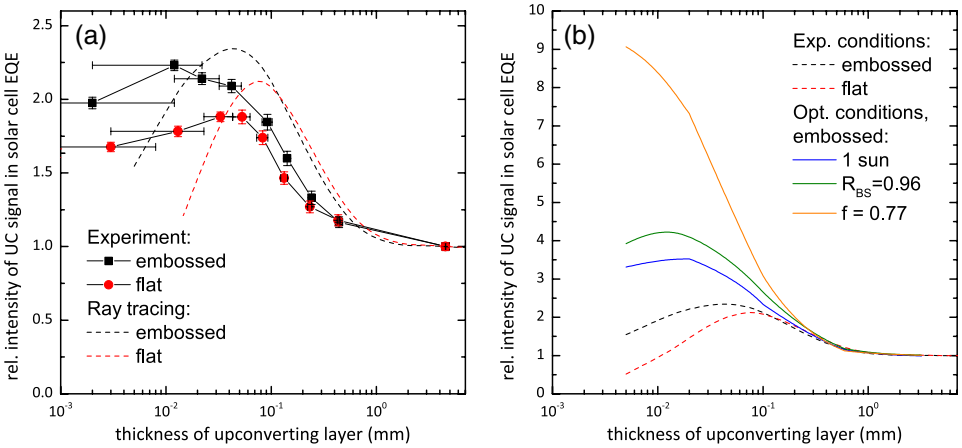

Fig. 5 (a) Development of the amplitude of the upconversion signal upon variation of the upconverter thickness in the presence of an embossed PTFE back reflector (normalized to the infinite limit), compared to ray tracing simulation. (b) Comparison of ray tracing results under experimental and optimized conditions of the embossment and illumination conditions (curves discussed in the text).

possible further gains, we again employed ray tracing simulations with the experimental parameters (listed in Table 1, simulation run B) as well as optimized parameters (listed in Table 1, simulation runs C1-C3). As visible from Fig. 5(a), there is a less good agreement of the simulation with the measured trend than for the silver reflector [Fig. 6(b)]. In particular, the decay of the UC yield for the smallest distances is not as drastic as predicted by the model, and the peak appears to be shifted to smaller distances. We attribute these deviations to the imperfect surface conditions of the PTFE film. First, as visible in Fig. 6, the surface area is rough on the $\sim$1 μm scale, particularly outside of the embossed dimples. While the rather smooth surface inside the embossments can be expected to provide mostly specular reflectance, the surface condition of the flat parts will lead to scattering, which may bring the optical behavior closer to a Lambertian characteristic. Under such circumstances, it is to be expected that the peak is shifted towards smaller distances as the effective path length of reflected light is increased by the scattering. Second, as inferred from micrometer gauge measurements taken at different spots on the reflector surface, macroscopic ripples of about 10 μm height were present on the PTFE reflector resulting from the gluing to the magnetic holder. This effectively prevents a complete closing of the gap, so the data points taken for nominal UC layer thicknesses $\leq$10 μm most likely correspond to larger thicknesses, which explains the missing decay for smallest distances.

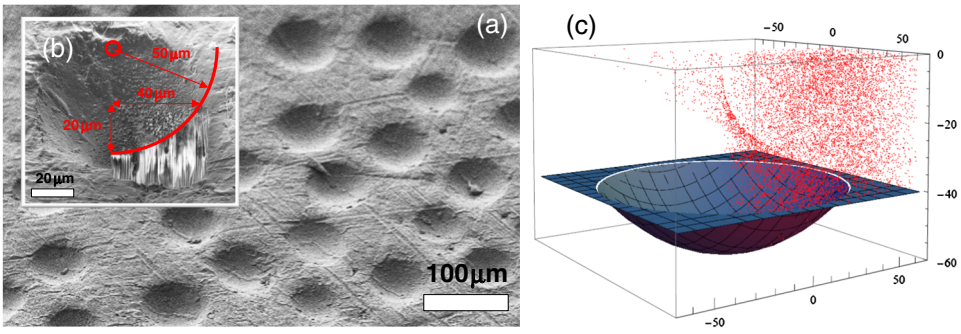

Fig. 6 (a) Spherical indentations in PTFE film as obtained by hot embossing of silica spheres. Successively, the films were Al-coated to provide a high reflectance. (b) Focused-ion-beam cut into the PTFE substrate with square geometry, imaged in tilted side view (perspective-corrected). The red line is a spherical arc with 50 μm radius (corresponding to the 100 μm diameter spheres used for embossing), illustrating the spherical shape of the embossments, and the roughly 20 μm indentation depth. (c) Ray tracing simulation for a 20 μm deep indented substrate (rays shown emerging from only one quadrant for clarity), illustrating the desired focusing effect. The units are μm.

Nonetheless, the difference in behavior between the embossed and flat parts of the reflector is captured well. The optimum thickness is shifted to smaller gaps for the embossed reflector, and it peaks at about 20% higher EQE improvement values. Although the beneficial effect of the embossment is small, it can be greatly enhanced by changing the geometry of the back reflector, and the measurement scheme. There are two aspects of the reflector which could be technologically optimized: the reflectivity and the density of dimples. Particularly the second quantity could be easily optimized by the preparation of a stamp with densely packed template spheres—in the present case, due to the moderate indentation depth of 15 to 20 μm, the surface fraction of dimples is only about 30%, which is far away from the geometrical limit. Further, reducing the illumination level from the about 50 suns practically needed for a good signal-to-noise ratio in the EQE measurement to the solar cell-relevant 1 sun illumination might also increase the UC yield as it is to be expected that the high pump power is already driving the bulk of the UC solution into/close to the linear regime. In such case, local concentration of light has a negligible/diminished effect, while for low illumination conditions—where the UC bulk is in the quadratic regime—the focusing has a much higher impact as the local UC efficiency can be greatly enhanced. We explored the significance of these three parameters in the ray tracing model described above. In a first step, the illumination density was reduced to 1 sun, to capture the device-relevant regime. This leads to an increase of the UC yield enhancement as compared to the infinite limit (single pass of light, no focusing) from 2.2 to about 3.5 [blue curve in Fig. 5(b)]. Increasing the back reflector reflectivity from 0.88 as realistic for Al to 0.96 as measured for the Ag reflector pushes the enhancement factor to about 4.5. The largest effect is observed for changing the area fraction of the embossments, which was increased from the experimentally realized 1/3 to 0.77. The latter value is the largest obtainable with the chosen square geometry of the ray tracing simulation volume, and is reasonably close to the absolute maximum of 0.91 represented by the hexagonal closest packing of circles. This leads to an enhancement factor of up to nine as compared to the infinite limit, which means that a structured back reflector with good reflectance placed at an optimum distance can increase the UC yield by almost an order of magnitude. This is a very significant result given the simple structure of the reflective medium, which is compatible with large-area processing.

3.4 *Overall EQE Improvement by the Back Reflector*

The last aspect we discuss in the present study is the impact of the back reflector on the overall EQE of the solar cell. In Fig. 7 we plot the EQE curves of the a-Si:H solar cell with a simple Lambertian back scattering layer (white paint) coated onto the glass substrate, as compared to the presence of the UC unit and (i) PTFE back reflector in the infinite limit, (ii) flat coated PTFE back reflector at optimum position, and (iii) embossed PTFE back reflector at optimum position. It is clearly visible that in the presence of the thick UC layer, the solar cell performs worst.

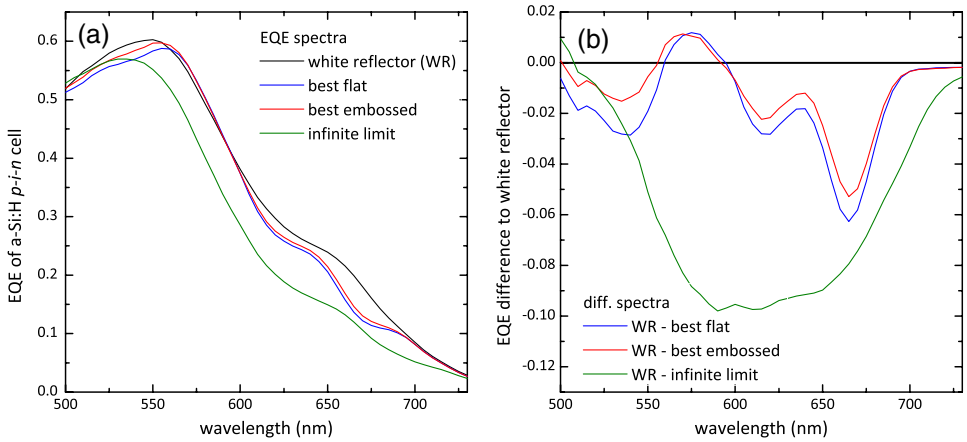

Fig. 7 (a) EQE curves of a-Si:H *p-i-n* cell in the presence of a Lambertian back reflector, compared to upconverter units comprising a flat or structured specular back reflector at optimum distance, or in the infinite limit. (b) Difference curves of EQEs from panel a.

Across the entire range of 550 to 700 nm, where the solar cell transmits a considerable fraction of light Fig. 2(c), but also has a nonzero EQE, the infinite limit is inferior to the white back reflector by up to 10%. This is due to the fact that apart from the fraction of the light that is upconverted, most of the transmitted photons are lost as the UC solution is optically thick over the entire visible range due to the high absorptivity of the sensitizer molecules. At the UC quantum efficiency presently being <1%,[15] only a small fraction of the photons entering the UC unit is re-radiated towards the solar cell.

It was shown above that the UC efficiency benefits greatly in the presence of a (structured) back reflector due to concentration of the incident light. Indeed, also the overall solar cell response is greatly improved by the presence of the back reflector, as can be seen from Fig. 7. Both the flat and structured back reflectors greatly diminish the EQE losses as compared to the infinite limit, with the main features persisting in the EQE difference spectra being peaks around 530, 620, and 670 nm. These coincide with the main absorption bands of rubrene (530 nm) and PQ_4Pd (620 and 670 nm), Fig. 2(c). Thus it can be concluded that the presence of the upconverter still leads to an overall loss of solar cell efficiency when compared to a Lambertian back reflector. Although disappointing, this is not surprising at the presently still low UC quantum efficiency.

Nonetheless, steps toward increasing the UC yield have been proposed that include concentration of the sensitizer species,[15,22–27] and molecular engineering.[22,28] This paper highlighted micro-optical means for local light concentration as an important additional component means for the increase of the UC yield, demonstrating a possible order-of-magnitude increase of the UC yield by a deliberately placed structured back-reflector.

4 Conclusions

In conclusion, we have analyzed the impact of the optical design of photochemical upconverters on the performance of a-Si:H *p-i-n* solar cells. We varied the thickness of the upconverting layer in the presence of a flat or microstructured back reflector, demonstrating a more than two-fold gain in the photocurrent contribution from UC, when a focusing microstructured back reflector is positioned at an optimum distance to the solar cell. Then, the upconverting medium is restrained to a thin layer, which allows the photons outside of the absorption range of the UC unit to efficiently be coupled back into the solar cell. The micro-focusing on the other hand improves the UC yield considerably, with ray tracing simulations promising an up to nine-fold gain for an optimized back reflector design. Although the presently achievable UC quantum yields are not sufficient for the upconverter unit to compete with a Lambertian back-reflector (being the "industry standard" for thin-film solar cell back-sides), the strategies highlighted in this paper may contribute significantly towards pushing UC to device-relevant photocurrent augmentation, in combination with increased sensitizer concentration and broadened absorption characteristics.

Acknowledgments

T. F. S. acknowledges the Alexander von Humboldt-Foundation for a Feodor Lynen fellowship. Y. C. acknowledges The University of Sydney for a Henry, Bertie and Florence Mabel Gritton Scholarship. K. L. is indebted to the Deutsche Forschungsgemeinschaft (DFG) for grant 583727 which initiated this German-Australian bilateral cooperation. We thank A. Stanco and Lastek for the gift of the 670 nm diode laser, M. Kaegi for making the solar cell holder, and T. Hänel as well as S. Kirner (PVComB) for EQE measurements. This research project is funded by the Australian Solar Institute (A-023), with contributions from The New South Wales Government and The University of Sydney. Aspects of this research were supported under Australian Research Council's Discovery Projects funding scheme (DP110103300 to T.W.S., DP1092560 to M. J. C.). Equipment was purchased with support from the Australian Research Council (LE0668257). The work related to the solar cell preparation at HZB was funded by the BMBF and the state government of Berlin (SENBWF) in the framework of the program "Spitzenforschung und Innovation in den NeuenLändern" (03IS2151).

References

1. W. Shockley and H. J. Queisser, "Detailed balance limit of efficiency of p-n junction solar cells," *J. Appl. Phys.* **32**(3), 510–519 (1961), http://dx.doi.org/10.1063/1.1736034.
2. M. C. Hanna and A. J. Nozik, "Solar conversion efficiency of photovoltaic and photoelectrolysis cells with carrier multiplication absorbers," *J. Appl. Phys.* **100**(7), 074510 (2006), http://dx.doi.org/10.1063/1.2356795.
3. L. C. Hirst and N. J. Ekins-Daukes, "Fundamental losses in solar cells," *Prog. Photovolt: Res. Appl.* **19**(3), 286–293 (2011), http://dx.doi.org/10.1002/pip.1024.
4. T. Schmidt and M. Tayebjee, *Comprehensive Renewable Energy*, A. Sayigh, Ed., pp. 533–548, Elsevier, Oxford (2012).
5. M. A. Green, *Third Generation Photovoltaics: Advances Solar Energy Conversion*, Springer-Verlag, Heidelberg (2003).
6. T. Trupke, M. A. Green, and P. Würfel, "Improving solar cell efficiencies by up-conversion of sub-band-gap light," *J. Appl. Phys.* **92**(7), 4117–4122 (2002), http://dx.doi.org/10.1063/1.1505677.
7. J. de Wild et al., "Upconverter solar cells: materials and applications," *Energy Environ. Sci.* **4**(12), 4835–4848 (2011), http://dx.doi.org/10.1039/c1ee01659h.
8. B. M. van der Ende, L. Aarts, and A. Meijerink, "Lanthanide ions as spectral converters for solar cells," *Phys. Chem. Chem. Phys.* **11**(47), 11081–11095 (2009), http://dx.doi.org/10.1039/b913877c.
9. A. Shalav et al., "Application of $NaYF_4$: Er^{3+} up-converting phosphors for enhanced near-infrared silicon solar cell response," *Appl. Phys. Lett.* **86**(1), 013505 (2005), http://dx.doi.org/10.1063/1.1844592.
10. S. Baluschev et al., "Up-conversion fluorescence: noncoherent excitation by sunlight," *Phys. Rev. Lett.* **97**(14), 143903 (2006), http://dx.doi.org/10.1103/PhysRevLett.97.143903.
11. A. Shalav, B. S. Richards, and M. A. Green, "Luminescent layers for enhanced silicon solar cell performance: up-conversion," *Sol. Energ. Mater. Sol. C* **91**(9), 829–842 (2007), http://dx.doi.org/10.1016/j.solmat.2007.02.007.
12. J. de Wild et al., "Enhanced near-infrared response of a-Si:H solar cells with β-$NaYF_4$: Yb^{3+} (18%), Er^{3+} (2%) upconversion phosphors," *Sol. Energ. Mater. Sol. C.* **94**(12), 2395–2398 (2010), http://dx.doi.org/10.1016/j.solmat.2010.08.024.
13. Y. Y. Cheng et al., "Improving the light-harvesting of amorphous silicon solar cells with photochemical upconversion," *Energy Environ. Sci.* **5**(5), 6953–6959 (2012), http://dx.doi.org/10.1039/c2ee21136j.
14. T. F. Schulze et al., "Photochemical upconversion enhanced solar cells: effect of a back reflector," *Aust. J. Chem.* **65**(5), 480–485 (2012), http://dx.doi.org/10.1071/CH12117.
15. T. F. Schulze et al., "Efficiency enhancement of organic and thin-film silicon solar cells with photochemical upconversion," *J. Phys. Chem. C* **116**(43), 22794–22801 (2012), http://dx.doi.org/10.1021/jp309636m.
16. Y. Cheng et al., "Kinetic analysis of photochemical upconversion by triplet–triplet annihilation: beyond any spin statistical limit," *J. Phys. Chem. Lett.* **1**(12), 1795–1799 (2010), http://dx.doi.org/10.1021/jz100566u.
17. W. Zou et al., "Broadband dye-sensitized upconversion of near-infrared light," *Nat. Photon.* **6**(8), 560–564 (2012), http://dx.doi.org/10.1038/nphoton.2012.158.
18. A. Monguzzi et al., "Upconversion-induced fluorescence in multicomponent systems: Steady-state excitation power threshold," *Phys. Rev. B.* **78**(19), 195112 (2008), http://dx.doi.org/10.1103/PhysRevB.78.195112.
19. Y. Y. Cheng et al., "On the efficiency limit of triplet–triplet annihilation for photochemical upconversion," *Phys. Chem. Chem. Phys.* **12**(1), 66–71 (2010), http://dx.doi.org/10.1039/b913243k.
20. A. Haefele et al., "Getting to the (square) root of the problem: how to make noncoherent pumped upconversion linear," *J. Phys. Chem. Lett.* **3**(3), 299–303 (2012), http://dx.doi.org/10.1021/jz300012u.

21. S. Baluschev et al., "Metal-enhanced up-conversion fluorescence: effective triplet-triplet annihilation near silver surface," *Nano Lett.* **5**(12), 2482–2484 (2005), http://dx.doi.org/10.1021/nl0517969.
22. T. Khoury and M. J. Crossley, "A strategy for the stepwise ring annulation of all four pyrrolic rings of a porphyrin," *Chem. Commun.* **46**(46), 4851–4853 (2007), http://dx.doi.org/10.1039/b714612d.
23. A. Monguzzi, R. Tubino, and F. Meinardi, "Upconversion-induced delayed fluorescence in multicomponent organic systems: role of dexter energy transfer," *Phys. Rev. B.* **77**(15), 155122 (2008), http://dx.doi.org/10.1103/PhysRevB.77.155122.
24. D. Jucius et al., "Hot embossing of PTFE: towards superhydrophobic surfaces," *Appl. Surf. Sci.* **257**(6), 2353–2360 (2011), http://dx.doi.org/10.1016/j.apsusc.2010.09.102.
25. J.-H. Kim et al., "High efficiency low-power upconverting soft materials," *Chem. Mater.* **24**(12), 2250–2252 (2012), http://dx.doi.org/10.1021/cm3012414.
26. P. B. Merkel and J. P. Dinnocenzo, "Low-power green-to-blue and blue-to-UV upconversion in rigid polymer films," *J. Lumin* **129**(3), 303–306 (2009), http://dx.doi.org/10.1016/j.jlumin.2008.10.013.
27. R. R. Islangulov et al., "Noncoherent low-power upconversion in solid polymer films," *J. Am. Chem. Soc.* **129**(42), 12652–12653 (2007), http://dx.doi.org/10.1021/ja075014k.
28. V. Yakutkin et al., "Towards the IR limit of the triplet–triplet annihilation-supported up-conversion: tetraanthraporphyrin," *Chem. Eur. J.* **14**(32), 9846–9850 (2008), http://dx.doi.org/10.1002/chem.v14:32.

Tim F. Schulze obtained his diploma in physics from ETH Zurich, in 2007. His PhD in physics was awarded by Technical University Berlin in 2011 based on his thesis on silicon heterojunctions for solar cell applications which was prepared at Helmholtz-Centre Berlin for Materials and Energy. Since 2011, he has been a Feodor-Lynen Postdoc of the Alexander-von-Humboldt foundation at the University of Sydney, working on the application of photochemical upconversion to solar cells. His research interests include hybrid and heterojunction solar cell concepts as well as spectral conversion for solar energy applications.

Klaus Lips is head of the Energy Materials In-Situ Laboratory Berlin at HZB and professor for analytics for photovoltaics at the Free University Berlin. His research activities comprise basic as well as application-oriented projects in the field of thin-film photovoltaics. He has 20 years of experience in the characterization of thin film materials and solar cells.

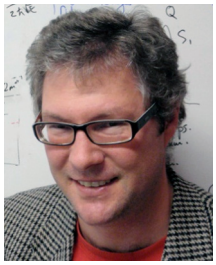

Timothy W. Schmidt is associate professor in chemistry at the University of Sydney. After gaining his BSc and the University Medal from the University of Sydney, he undertook a PhD in femtosecond spectroscopy in Cambridge (UK), before embarking on postdoctoral work in Basel (Switzerland). He was the recipient of the 2010 Coblentz Award.

Biographies and photographs of other authors are not available.